Dynamic State Estimation Based Protection of Microgrid Circuits

Yu Liu, *Student Member, IEEE,* A. P. Sakis Meliopoulos, *Fellow, IEEE*
Rui Fan, *Student Member, IEEE,* and Liangyi Sun, *Student Member, IEEE*
School of Electrical and Computer Engineering, Georgia Institute of Technology,Atlanta, Georgia 30332-0250, USA
Email: yliu400@gatech.edu

***Abstract*—Microgrid protection presents challenges because of the presence of inverter interfaced resources which results in insufficient separation between fault and load currents. This paper uses the Dynamic State Estimation (DSE) based protection (EBP) method for the protection of microgrid components. The paper demonstrates that this method provides a reliable protection system as opposed to traditional methods. Specifically, we verify that traditional protection functions such as overcurrent, distance etc. fail to provide selectivity in protection of microgrids. The EBP method can be viewed as an evolution of current differential protection and requires GPS synchronization if measurements come from different metering devices. The method mainly determines whether the measurements are consistent with the model of the protection zone by use of the chi-square test. Numerical simulations prove that the method can correctly respond to different fault types and locations. The method works equally well for three-phase balanced or unbalanced systems, two-phase or single-phase systems, and radial or networked microGrids.**

***Key words*—Microgrid component protection, Dynamic State Estimation (DSE), Estimation Based Protection (EBP), Loss of measurements**

I Introduction

MICROGRID is one of the methods to integrate large numbers of Distributed Generation (DG) sources without significant impact to the main grid [1-3], and brings promising environmental and economic benefits. In addition, in case of a disturbance in the main grid, the microgrid can automatically island (for example by use of a static switch) so the customers will not experience any power outages [4]. Microgrids thus increase the reliability of power supply to customers.

Microgrids must be protected against faults. Their characteristics influence the applicability of legacy protection schemes. Specifically, microgrids have the following characteristics, as related to protection scheme requirements: (a) significant difference between fault currents contributed by the main grid and by DG sources, since DG sources are interfaced via inverters which limit fault currents, (b) short length circuits operating at relatively low voltages, and (c) variable and intermittent generation resulting in frequent changes of the microgrid network. These characteristics seriously comprimize the effectiveness of legacy protection functions.

The paper discusses the limitation of traditional protection schemes as applied to microgrid systems, such as the one shown in Figure 1, where the microgrid operates in the grid-connected mode. Here we have micro power sources such as PVs and wind turbines, and bulk power sources in the main grid. The components of the microgrid are connected via low voltage cables.

Consider the application of traditional protection to the circuit I-II (protected circuit) of the microgrid of Figure 1. The following discussion applies.

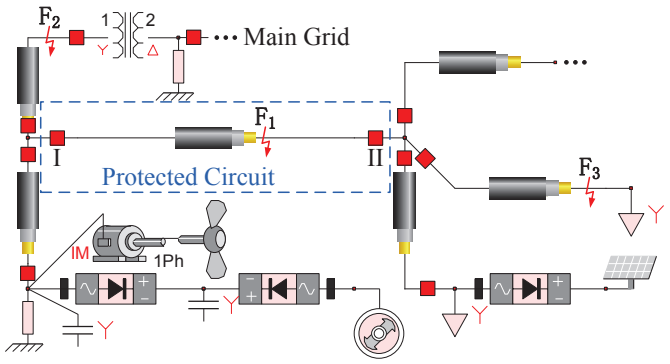

Figure 1. Example Microgrid System

Directional overcurrent protection: it is required because of bi-directional power flow in microgrid circuits. Three main problems affect the performance of directional overcurrent protection: (a) fault currents vary as the number of generating sources connected to the system changes with time, (b) fault current level variability along microgrid circuits is limited, and (c) in case of islanding the fault current level may be comparable to load currents. These issues make the setting selection process for legacy directional overcurrent protection schemes very difficult, i.e. it is almost impossible to provide the required selectivity.

Distance protection: it can theoretically avoid the influence of source variations, since it only monitors the impedance between the measurement and the fault position. However, because microgrid circuits are typically short, distance protection cannot operate securely and dependably, a well known limitation for short circuits. Another issue is that distance protection works well for three-phase circuits that are near symmetric and where load currents are much lower than fault currents. Microgrid circuits may not meet these two requirements leading to mis-operations. Detail analysis by example will be given in part III.

Differential protection: it is effective in protecting microgrid circuits [5-7]. Since most microgrid circuits are short, differential protection can be implemented with dedicated

978-1-4673-8040-9/15/$31.00 ©2015 IEEE

wiring resulting in a reliable protection system. If use of communication channel is required, differential protection will be quite vulnerable to all issues associated with communication failures [8]. For security, differential protection settings are typically desensitized to avoid nusance trippings which results in unreliability for high impedance faults.

To solve the above issues, Dynamic State **E**stimation **B**ased **P**rotection (EBP) method (a.k.a setting-less protection) is introduced [9-12]. It does not need complicated settings and no coordination is required with other protection functions. The algorithm examines the consistency between the measurements and the dynamic model of the protection zone. The EBP has been inspired from differential protection which simply monitors Kirchoff's current law of a protection zone. EBP extents this concept to monitor all physical laws obeyed by the protection zone, and therefore will not be affected by external variations such as frequent changes of sources or loads. Additionally, the EBP method performs more reliably than differential protection since it uses a realistic and dynamic protection zone model and more information in terms of voltage measurements and other quantities. Note that all physical laws that a protection zone must obey are captured by the dynamic model of the protection zone.

This paper advocates the use of Estimation Based Protection (EBP) for all components of a microgrid. To meet the space limitations of a technical paper, we demonstrate the applicability and advantages of EBP on microgrid circuits only (same can be shown for any microgrid component). In this paper, we first build the dynamic model for the protected microgrid circuit. Next for specific events we apply the EBP protection scheme and compare the results with the performance of traditional protection methods such as distance protection and differential protection.

II Dynamic State Estimation Based Protection

EBP can be thought of as a generalization of current differential protection as described before. Specifically it uses measurements of current, voltage and any other available measurements in the protection zone and determines whether the measurements are consistent with the dynamical model of the protection zone which expresses all the physical laws that must be obeyed by the protection zone. Therefore the first step is the dynamic model of the protection zone which is presented next. The consistency of the measurements and the dynamic model is determined by the application of dynamic state estimation. The application of EBP to circuits is presented next.

A. Microgrid Circuit Model and Measurements

The dynamic model for a short circuit is shown in Figure 2. $\mathbf{R}$, $\mathbf{L}$, $\mathbf{C}$ and $\mathbf{G}$ are the resistance, inductance, capacitance and stabilizing conductance matrices of the the circuit.

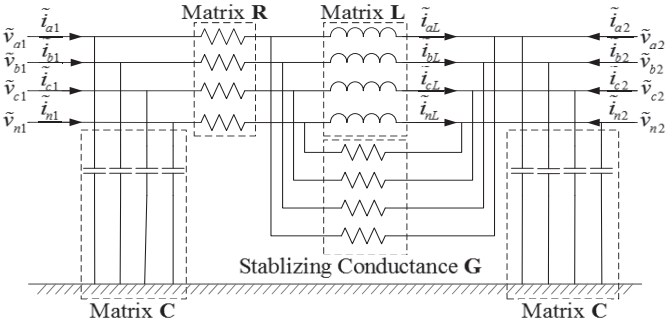

Figure 2. π-equivalent Circuit Model

The following differential equations in matrix form apply:

$$\left[\tilde{\mathbf{i}}_1 \quad \tilde{\mathbf{i}}_2 \quad \mathbf{0}\right]^{\mathrm{T}} = \mathbf{A}\cdot\left[\tilde{\mathbf{v}}_1 \quad \tilde{\mathbf{v}}_2 \quad \tilde{\mathbf{i}}_L\right]^{\mathrm{T}} + \mathbf{B}\cdot\frac{d}{dt}\left[\tilde{\mathbf{v}}_1 \quad \tilde{\mathbf{v}}_2 \quad \tilde{\mathbf{i}}_L\right]^{\mathrm{T}} \quad (1)$$

where

$$\tilde{\mathbf{i}}_j = \left[\tilde{i}_{aj} \quad \tilde{i}_{bj} \quad \tilde{i}_{cj} \quad \tilde{i}_{nj}\right]^T \quad \tilde{\mathbf{v}}_j = \left[\tilde{v}_{aj} \quad \tilde{v}_{bj} \quad \tilde{v}_{cj} \quad \tilde{v}_{nj}\right]^T \quad (j = 1,2)$$

$$\tilde{\mathbf{i}}_L = \left[\tilde{i}_{aL} \quad \tilde{i}_{bL} \quad \tilde{i}_{cL} \quad \tilde{i}_{nL}\right]^T$$

$$\mathbf{A} = \begin{bmatrix} \mathbf{0} & \mathbf{0} & \mathbf{I}_{4\times4} \\ \mathbf{0} & \mathbf{0} & -\mathbf{I}_{4\times4} \\ -\mathbf{I}_{4\times4} & \mathbf{I}_{4\times4} & \mathbf{R} \end{bmatrix} \quad \mathbf{B} = \begin{bmatrix} \mathbf{C} & \mathbf{0} & \mathbf{G}\cdot\mathbf{L} \\ \mathbf{0} & \mathbf{C} & -\mathbf{G}\cdot\mathbf{L} \\ \mathbf{0} & \mathbf{0} & \mathbf{R}\cdot\mathbf{G}\cdot\mathbf{L}+\mathbf{L} \end{bmatrix}$$

and $\mathbf{I}_{4\times4}$ is the 4×4 identity matrix.

Assume the sampling interval is Δt. Upon the quadratic integration of the above model with time step $2\Delta t$, the differential equations are converted into algebraic equations [13]. The results are:

$$\left[\mathbf{I}(t) \quad \mathbf{I}(t-\Delta t)\right]^{\mathrm{T}} = \mathbf{Y}\cdot\left[\mathbf{X}(t) \quad \mathbf{X}(t-\Delta t)\right]^{\mathrm{T}} - \mathbf{b}_{eq}(t) \quad (2)$$

$$\mathbf{b}_{eq}(t) = \mathbf{M}\cdot\mathbf{I}(t-2\Delta t) + \mathbf{N}\cdot\mathbf{X}(t-2\Delta t) \quad (3)$$

where $\mathbf{I}(t) = \left[\mathbf{i}_1(t) \quad \mathbf{i}_2(t) \quad \mathbf{0}\right]^{\mathrm{T}}$ $\mathbf{X}(t) = \left[\mathbf{v}_1(t) \quad \mathbf{v}_2(t) \quad \mathbf{i}_L(t)\right]^{\mathrm{T}}$

$$\mathbf{Y} = \begin{bmatrix} \mathbf{A}+2\mathbf{B}/\Delta t & -4\mathbf{B}/\Delta t \\ \mathbf{B}/(4\Delta t) & \mathbf{A}+\mathbf{B}/\Delta t \end{bmatrix} \quad \mathbf{N} = \begin{bmatrix} -2\mathbf{B}/\Delta t+\mathbf{A} \\ 5\mathbf{B}/(4\Delta t)-\mathbf{A}/2 \end{bmatrix} \quad \mathbf{M} = \begin{bmatrix} -\mathbf{I}_{12\times12} \\ 0.5\mathbf{I}_{12\times12} \end{bmatrix}$$

$\mathbf{I}_{12\times12}$ is the 12×12 identity matrix, and

the definition of $\mathbf{i}_1(t)$, $\mathbf{i}_2(t)$, $\mathbf{v}_1(t)$, $\mathbf{v}_2(t)$ and $\mathbf{i}_L(t)$ are similar as before, except that they represent the instantaneous values of the corresponding measurements at time t.

Equations (2) and (3) express the circuit terminal currents as functions of the circuit states, i.e. two side voltages and inductance currents.

The measurements are: $\tilde{i}_{aj}$, $\tilde{i}_{bj}$, $\tilde{i}_{cj}$ and $\tilde{i}_{nj}$ are 3-phase and neutral currents on side j ($j = 1,2$); $\tilde{v}_{aj}$, $\tilde{v}_{bj}$, $\tilde{v}_{cj}$ and $\tilde{v}_{nj}$ are 3-phase and neutral voltages on side j ($j = 1,2$); and $\tilde{i}_{aL}$, $\tilde{i}_{bL}$, $\tilde{i}_{cL}$ and $\tilde{i}_{nL}$ are 3-phase and neutral currents through the circuit inductances. The measurements are expressed as functions of the circuit states:

$$\breve{\mathbf{z}}(t) = \mathbf{H}\cdot\mathbf{x}(t) - \mathbf{B}_{eq}(t) \quad (4)$$

where the measurements vector $\breve{\mathbf{z}}(t)$ contains 40 elements; the states vector $\mathbf{x}(t)$ contains 24 elements; and

$$\breve{\mathbf{z}}(t)=\begin{bmatrix}\breve{\mathbf{v}}_1(t) & \breve{\mathbf{v}}_2(t) & \breve{\mathbf{v}}_1(t-\Delta t) & \breve{\mathbf{v}}_2(t-\Delta t) & \mathbf{I}(t) & \mathbf{I}(t-\Delta t)\end{bmatrix}^{\mathrm{T}}$$

$$\mathbf{x}(t)=\begin{bmatrix}\mathbf{X}(t)\\ \mathbf{X}(t-\Delta t)\end{bmatrix}^{\mathrm{T}} \quad \mathbf{H}=\begin{bmatrix}\mathbf{T} & \mathbf{0} & \mathbf{0} & \mathbf{0} & \mathbf{0} & \mathbf{0}\\ \mathbf{0} & \mathbf{T} & \mathbf{0} & \mathbf{0} & \mathbf{0} & \mathbf{0}\\ \mathbf{0} & \mathbf{0} & \mathbf{0} & \mathbf{T} & \mathbf{0} & \mathbf{0}\\ \mathbf{0} & \mathbf{0} & \mathbf{0} & \mathbf{0} & \mathbf{T} & \mathbf{0}\\ & & & \mathbf{Y} & & \end{bmatrix} \quad \mathbf{B}_{eq}(t)=\begin{bmatrix}\mathbf{0}\\ \mathbf{0}\\ \mathbf{0}\\ \mathbf{0}\\ \mathbf{b}_{eq}(t)\end{bmatrix}$$

B. Dynamic State Estimation and Chi-square Test

The dynamic state estimation is formulated as the following weighted least square optimization problem:

$$Min \quad J=\left(\breve{\mathbf{z}}(t)-\mathbf{H}\cdot\mathbf{x}(t)+\mathbf{B}_{eq}(t)\right)^{T}\mathbf{W}\left(\breve{\mathbf{z}}(t)-\mathbf{H}\cdot x(t)+\mathbf{B}_{eq}(t)\right) \quad (5)$$

where $\mathbf{W}$ is the weight matrix of the measurements:

$$\mathbf{W}=\mathrm{diag}\left\{1/\sigma_1^{\,2},1/\sigma_2^{\,2},\cdots,1/\sigma_n^{\,2}\right\} \quad (6)$$

σ_i $(i=1\sim 40)$ are standard deviations of measurement error.

The computational steps are:

(a) Compute the best estimation of the circuit states. The best estimate $\hat{\mathbf{x}}(t)$ of the overdetermined set of equations (4) is:

$$\hat{\mathbf{x}}(t)=(\mathbf{H}^{\mathrm{T}}\mathbf{W}\mathbf{H})^{-1}\mathbf{H}^{\mathrm{T}}\mathbf{W}\left(\mathbf{z}(t)+\mathbf{B}_{\mathrm{eq}}(t)\right) \quad (7)$$

(b) The residuals, or the difference between the real measurements and the estimated measurements are:

$$\hat{\mathbf{r}}(t)=\mathbf{H}\cdot\hat{\mathbf{x}}(t)-\mathbf{B}_{\mathrm{eq}}(t)-\breve{\mathbf{z}}(t) \quad (8)$$

(c) If the measurements match the dynamic model quite well, the residuals should be comparable to the measurement error. If they are much larger than the metering errors, the model has changed and there exists some fault in the system. To quantify the consistency, the normalized residual $\hat{\mathbf{s}}(t)$ and the confidence level $p(t)$ are calculated by:

$$\hat{\mathbf{s}}(t)=\sqrt{\mathbf{W}}\cdot\hat{\mathbf{r}}(t) \quad (9)$$

$$\zeta(t)=\hat{\mathbf{s}}(t)^{\mathrm{T}}\hat{\mathbf{s}}(t) \quad (10)$$

$$p(t)=P\left(\chi^2\geq\zeta(t)\right)=1-P\left(\zeta(t),v\right) \quad (11)$$

where $P\left(\zeta(t),v\right)$ is the probability of χ^2 distribution of $\chi^2\leq\zeta(t)$, with v degree of freedom (m-n). This process is also known as the chi-square test [14]. A high confidence level near 100% describes a good consistency between the measurements and the circuit model. If the confidence level is low, we can conclude that some fault has occurred within the protection zone. The trip signal issued only when the intergral of the confidence level over a user selected time remains small.

III ILLUSTRATIVE RESULTS

An example test system has been used to illustrate the EBP relay operation and compare it to the performance of legacy protection functions. The example system and events follow.

A. System Configuration

The example microgrid circuit is a 480 V circuit and is illustrated in Figure 1. The protected circuit is circuit I-II. The cable structure of the circuit is shown in Figure 3. Detail system parameters are given in Table 1. It is important to point out that for the legacy protection function of distance protection the positive, negative and zero sequence model is used but for the EBP the asymmetric dynamic model of the circuit is used. The sampling frequency is 5 kilo-samples per second (sampling period of 200 microsec).

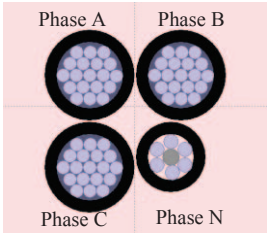

Figure 3. Cable Structure

Table 1. Example Microgrid Circuit Parameters

Object	*Parameter*	*Value*
System	Line to line voltage	480 *V*
	Fundamental frequency	60 *Hz*
	Length of the protected circuit	400 feet
Protected Circuit	Positive (Negative) sequence	0.0475+ *j* 0.0152 Ω
	Zero sequence	0.1747+ *j* 0.1595 Ω

B. EBP Measurements Definitions

In this part the measurement definitions of EBP method is introduced. We have three-phase current and three-phase voltage actual measurements at both sides of the circuit, i.e. 24 actual measurements. The standard deviations of these actual measurements are chosen as 0.01 p.u. on a 480 V (L-L) and 142 kVA (3-phase) base system. In addition there are 16 pseudo and virtual measurements as follows: (a) 8 pseudo voltage and current measurements. These measurements represent the voltages and currents of the neutral conductor where meters are not typically installed. Normally, the voltages and currents are near zero. However, with an external fault at F_3, the neutral current will be very large because of the large fault current contributed by the main grid. Moreover, the unbalanced three-phase loads will also lead to substantial neutral current. To securely prevent mis-opeations during above situations, we can simply set these measurements to zero with very large standard deviations, eg. 0.1 p.u. for neutral voltages and 0.5 p.u. for neutral currents. (b) 8 virtual voltage measurements. These measurements represent the two zero vectors ($\mathbf{0}$) in $\breve{\mathbf{z}}(t)$. We allow little variance of these measurements because they come from the zero sum of total voltages composed by the states of the system. Here we choose 0.001 p.u. as the standard deviation for the virtual measurements.

C. Simultaion Results

For this example system, various types of faults at different time and locations with different fault impedances have been considered. In this section, we present the results for the following events. **Event 1**: low impedance internal phase to neutral fault; **Event 2**: the same internal fault with unbalanced loads; **Event 3**: the same internal fault with the loss of one side current measurements. Note that in all the figures of EBP results,

three-phase currents at side II are chosen as an example, and actual measurements, estimated measurements, and confidence level are depicted in real time.

EVENT 1: An internal fault with 0.12 ohm impedance is simulated at 3.4s. The fault location is the midpoint of circuit I-II, i.e. 200 feet from side II.

Distance Protection Function, Event 1: The impedances as seen at the relay location II are depicted in Figure 4. Here the settings of zone 1, 2 and 3 are 80%, 125% and 260% of the circuit positive impedance, respectively. We can observe the following two facts. (a) The theoretical impedance already falls outside of the tripping characteristics of the relay, only with 0.12 ohm fault impedance. (b) The calculated impedance with asymmetric model falls further away, which proves that the effect of fault impedance is magnified by the fault current that is near to the load current. Therefore, even a low fault impedance may cause operation failure of the distance relay II.

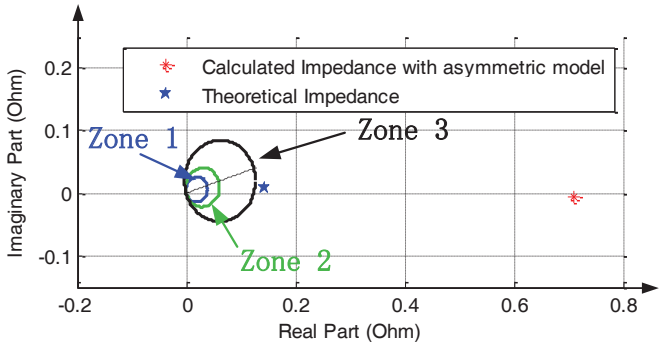

Figure 4. Distance Protection: Low Impedance Internal Fault

EBP Relay, Event 1: From the results in Figure 5, the EBP algorithm can correctly detect this internal fault. During this internal fault, the confidence level drops from 100% to 0%, which clearly indicates abnormality in the system.

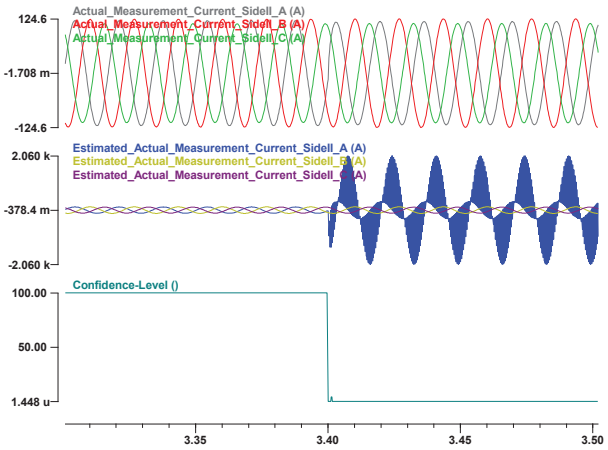

Figurte 5. EBP Results: Low Impedance Internal Fault

EVENT 2: In this event, three-phase unbalanced loads are applied to the system, where phase A has an additional 20% load compared with other two phases. The internal fault is the same as in Event 1.

Distance Protection Function, Event 2: The impedances as seen by relay II are shown in Figure 6. The settings are chosen the same as the distance relay in Event 1. We can see that the calculated impedance is even further away from the theoretical value, compared with the results in Figure 4. This extra error is caused by the unbalanced loads. Thus, the distance relay II may not correctly respond to this internal fault.

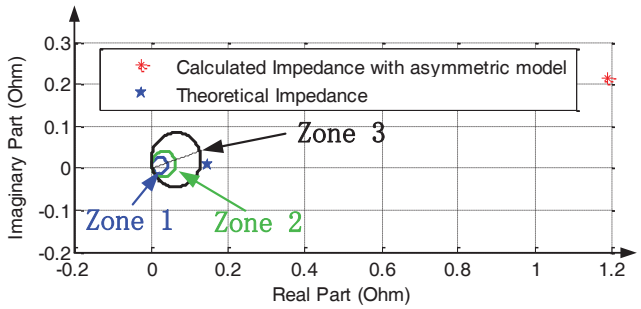

Figure 6. Distance Protection: Low Impedance Internal Fault with Unbalanced Loads

EBP Relay, Event 2: The EBP method can detect internal faults with unbalanced loads. Figure 7 shows that, the EBP algorithm retains 100% confidence level under normal but unbalanced operation and accurately detects the internal fault.

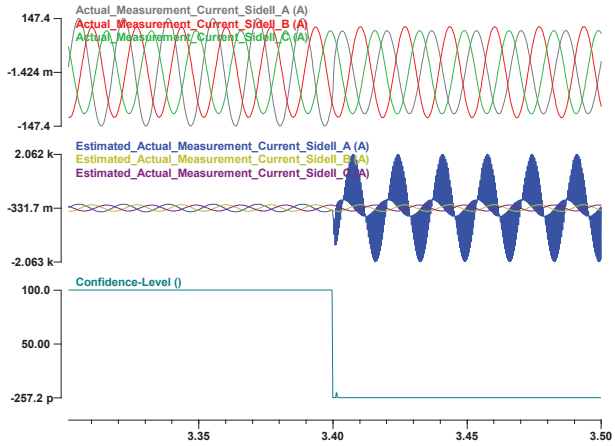

Figurte 7. EBP Results: Low Impedance Internal Fault with Unbalanced Loads

EVENT 3: This event represents the performance of line differential protection function and EBP relay with the loss of three-phase current measurements at side I. The internal fault is the same as in Event 1.

Line Differential Protection Function, Event 3: Figure 8 depicts the results of line differential relay (eg. SEL-387L) in the alpha plane. Here the ratio is calculated between the current phasors going into the circuit at side I and side II. The relay trips only when: (a) the phase currents exceed a threshold setting (in this case 1.2 p.u.); and (b) the ratio exits the restraint region. The settings of the restraint region are chosen as: outer radius: 6, inner radius: 1/6, and total angular extent: 195°. With the loss of current measurements at side 1, the ratio remains at zero and exits the restraint region. However, since the fault current is

similar as the load current and does not exceed the threshold, the differential relay will not trip during this internal fault.

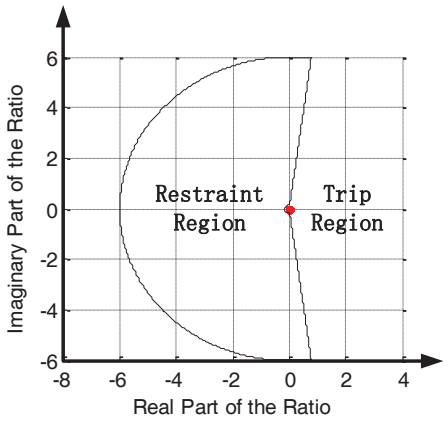

Figure 8. Differential Protection Results: Low Impedance Internal Fault with the Loss of One Side Current Measurements

EBP Relay, Event 3:Figure 9 depicts the result of EBP relay. We can see that the algorithm can still effectively detect the internal fault, even without one side current measurements.

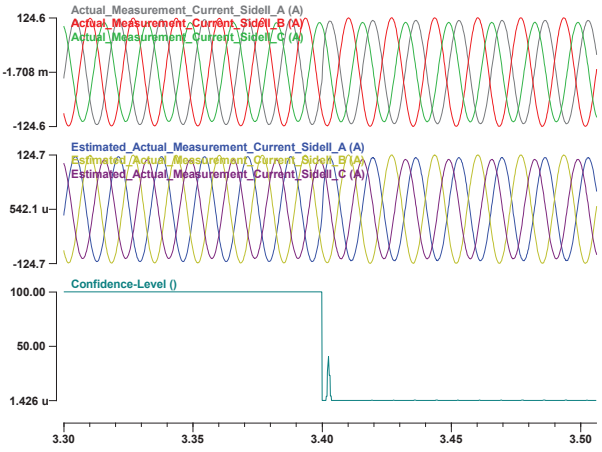

Figure 9. EBP Results: Low Impedance Internal Fault with the Loss of One Side Current Measurements

IV Conclusions

Microgrid is an effective way to integrate DG sources. As any electrical system, the microgrid must be protected against any possible fault condition. Traditional protection methods such as overcurrent and distance protection have limitations when applied to microgrid components because the circuits are short and fault current variability along the circuit is very small. The paper proposed a new Dynamic State **E**stimation **B**ased **P**rotection (EBP) algorithm where the consistency between measurements and the dynamic model of the protected zone is tested via the Dynamic State Estimation process. Several examples have been presented which indicate the following results of the EBP method:

(a) it can correctly respond to fault types and locations;

(b) it is immune to balanced or imbalanced conditions;

(c) it can tolerate some loss of measurements (communications).

While the paper presented examples for microgrid circuit protection only, the same method can be applied to any protection zone in the microgid, i.e. other microgrid components.

V Acknowledgment

This work is supported by PSERC and EPRI. Their support is greatly appreciated.

VI References

[1] R. H. Lasseter, “Microgrids,” in *Proc. IEEE Power Engineering Society Winter Meeting*, 2002, vol. 1, pp. 305–308

[2] R. H. Lasseter and P. Piagi, “Microgrid: A conceptual solution,” in *IEEE Proceeding of Power Electronics Specialists Conference*, Jun. 2004, pp. 4285–4290.

[3] N. Hatziargyriou, H. Asano, R. Iravani, and C. Marnay, “Microgrids,” in *IEEE Power Energy Mag*zine, vol. 5, no. 4, pp. 78–94, Jul./Aug. 2007.

[4] H. Nikkhajoei and R. Lasseter, “Microgrid protection,” in *IEEE Proceeding of Power Engineering Society General Meeting*, Tampa, FL, Jun. 24–28, 2007, pp. 1–6.

[5] E. Sortomme, S. S. Venkata, and J. Mitra, “Microgrid protection using communication-assisted digital relays,” *IEEE Transanction on Power Delivery*, vol. 25, no. 4, pp. 2789–2796, 2010.

[6] M. Dewadasa, et al., "Protection of microgrids using differential relays," in *Universities Power Engineering Conference (AUPEC)*, 2011 21st Australasian, 2011, pp. 1-6.

[7] T. S. Ustun, C. Ozansoy, and A. Zayegh, “Differential protection of microgrids with central protection unit support,” in *IEEE Region Ten Conference (TENCON)* Spring, 2013.

[8] Hatziargyriou, N., “Microgrid Protection,” in *Microgrids: Architectures and Control*. New York: Wiley, 2014, ch. 4, pp. 119-120.

[9] A. P. Meliopoulos, G. J. Cokkinides, Z. Tan, S. Choi, Y. Lee, and P. Myrda, “Setting-less protection: Feasibility study,” in *Proceeding of 2013 46th Hawaii International Conference on System Sciences (HICSS)*, Maui, HI, USA, Jan. 2013, pp. 2345–2353.

[10] E. Farantatos, G. K. Stefopoulos, G. J. Cokkinides, and A. P. S. Meliopoulos, "PMU-based dynamic state estimation for electric power systems," in *Proceeding of IEEE Power Engineering Society General Meeting*, 2009.

[11] R. Huang, E. Farantatos, G. J. Cokkinides, and A. P. S. Meliopoulos, "Substation based dynamic state estimator - numerical experiment," in *Proc. IEEE Power Engineering Society Transmission and Distribution Conference and Exposition*, New Orleans, 2010.

[12] A. P. S. Meliopoulos, G. J. Cokkinides, C. Hedrington, and T. L. Conrad, "The supercalibrator - A fully distributed state estimator," in *Proceeding of IEEE Power Engineering Society General Meeting*, 2010.

[13] A. P. Meliopoulos, G. J. Cokkinides, and G. K. Stefopoulos, "Quadratic Integration Method," in *Proceedings of the 2005 International Power System Transients Conference (IPST 2005)*, Montreal, Canada, 2005.

[14] F. C. Schweppe,R. D. Masiello, "A Tracking Static State Estimator," *IEEE Transactions on Power Apparatus and Systems*, vol. PAS-90, pp. 1025-1033, 1971.

VII Biographies

Yu Liu is now a Ph.D student in Georgia Tech. His research interests include protections of components in power system and microgrids.

A. P. Sakis Meliopoulos is a professor in Georgia Tech. He has made significant contributions to power system grounding, harmonics, protection and reliability assessment of power systems. He is the Chairman of the Georgia Tech Protective Relaying Conference, a Fellow of the IEEE and a member of Sigma Xi.

Rui Fan is now a Ph.D student in Georgia Tech. His research interests include power electronics, power system protection, and micro-grid operation.

Liangyi Sun is now a Ph.D student in Georgia Tech. His research interests include power system protection, transient stability and wind power control.